Lake Water Isotope Variation Linked with the In-Lake Water Cycle of the Alpine Bangong Co, Arid Western Tibetan Plateau

Authors: Wen, Rong, Tian, Lide, Liu, Fengjing, and Qu, Dongmei

Source: Arctic, Antarctic, and Alpine Research, 48(3) : 563-580

Published By: Institute of Arctic and Alpine Research (INSTAAR), University of Colorado

URL: https://doi.org/10.1657/AAAR0015-028

Arctic, Antarctic, and Alpine Research, Vol. 48, No. 3, 2016, pp. 563–580
DOI: http://dx.doi.org/10.1657/AAAR0015-028

Lake water isotope variation linked with the in-lake water cycle of the alpine Bangong Co, arid western Tibetan Plateau

Rong Wen[1,2,*], Lide Tian[1,3], Fengjing Liu[4], and Dongmei Qu[1]

[1]Key Laboratory of Tibetan Environment Changes and Land Surface Processes, Institute of Tibetan Plateau Research, Chinese Academy of Sciences, Building 3, Courtyard 16, Lin Cui Road, Chaoyang District, Beijing 100101, P.R. China
[2]University of Chinese Academy of Sciences, 19 A Yuquan Road, Shijingshan District, Beijing 100049, P.R. China
[3]CAS Center for Excellence in Tibetan Plateau Earth Sciences, Building 3, Courtyard 16, Lin Cui Road, Chaoyang District, Beijing, 100101, P.R. China
[4]Department of Agriculture and Environmental Science *and* Cooperative Research Program, Lincoln University, 820 Chestnut Street, Jefferson City, Missouri 65101, U.S.A.
[*]Corresponding author's email: wenrong@itpcas.ac.cn

A B S T R A C T

Water isotopes play an important role in the study of the alpine lake water budget and the hydrological cycle in the arid, far western Tibetan Plateau. These isotope records, derived from well-preserved sediments, are believed to reflect climatic and environmental changes. Using two years of $\delta^{18}O$ and δD data from precipitation, river water, underground water, and lake water at the long alpine lake Bangong (LBG), together with local meteorological observations in the arid western Tibetan Plateau, this study reveals that the $\delta^{18}O$ in the lake is over 10‰ more enriched than that in the local precipitation due to evaporation of the lake water. Spatial changes in both the lake water $\delta^{18}O$ and *d*-excess (= $\delta D - 8 * \delta^{18}O$) are apparent, ranging from ~–4.9‰ to +0.9‰ for $\delta^{18}O$, and –13.22‰ to –30.85‰ for *d*-excess, respectively, from east to west of the lakes. Simulation with the Craig-Gordon model shows that the isotopes in alpine inland lake water are controlled to a great extent by local relative humidity. Using a modified partly mixed isotope fractionation model, we rebuilt the spatial change of the evaporation/inflow (E/I) ratios from east to west of the lake. A quantitative estimation shows that the E/I ratio of the lake water increases from 0.73~0.83 in the eastern part and 0.90~0.93 in the western part of LBG. We also found that by assuming a full development of kinetic fractionation of the environmental vapor isotopes, our simulation result matched the observed spatial change for both $\delta^{18}O$ and *d*-excess, confirming the strong inland evaporation enrichment in the northern part of the plateau. This research may increase our understanding of inland water movement in the alpine Tibetan lakes, and also will improve our understanding of the lake sediment isotope record.

Introduction

Hydrological processes and the water cycle of lake water isotopes are widely used to determine water budget balances (Gat, 1996; Gibson, 2002; Gibson et al., 2002; Tian et al., 2008; Yuan et al., 2011) and the hydrological cycle (Grafenstein et al., 1996; Gat and Airey, 2006; Yao et al., 2007; Bowen et al., 2011). The Tibetan Plateau has the largest number of lakes in China (Wang, 1998) and is highly relevant to global climate dynamics and the Indian monsoon system (Immerzeel et al., 2010). Global climate change has accelerated the retreat of glaciers and permafrost thawing, which have be-

come the predominant sources of inflow for many expanding lakes (Yao et al., 2007; Ye et al., 2007; Zhou et al., 2013), thus leading to changes in lake water levels (Lu et al., 2005; Kropacek et al., 2012; Lei et al., 2014). Understanding the role that lakes at high elevations play in the seasonal and annual water balance and water cycle of the arid Tibetan Plateau, especially in the remote western alpine regions over the last three decades (Song et al., 2013, 2014; Zhang et al., 2013, 2014; Wu et al., 2014), is essential.

The heterogeneity of stable isotopes and chemical components caused by differences in hydrology and climatology can also be used to reconstruct paleoclimatic and paleoenvironmental changes (Fontes et al., 1996; Wang et al., 2002; Zhu et al., 2008, 2009). It has been shown that more negative values of carbonate $\delta^{18}O$ in the deglaciation stage reflect a cooling climate and a low evaporation rate (Gasse et al., 1991, 1996) or relationship with the Indian monsoon (Fontes et al., 1996). Recent studies have shown that there is still room for improvement in the understanding of isotopic processes, notably those leading to observed variations in the *d*-excess ($= \delta D - 8 * \delta^{18}O$) (Dansgaard, 1964) in precipitation in polar and high mountain regions (Masson-Delmotte et al., 2008; Yu et al., 2007, 2009). The *d*-excess that has been calculated as an index indicates that the influence of kinetic fractionation (evaporation) can be compared with equilibrium fractionation on water isotopes. Lower *d*-excess in lakes generally indicates more evaporation. Both $\delta^{18}O$ and *d*-excess could provide powerful tools for observing and quantifying the spatially integrated effects of water cycle processes within watersheds and air sheds (Bowen et al., 2011; Brooks et al., 2014; Gibson et al., 2016).

The isotope fraction process between lakes and precipitation is in equilibrium, and the Craig-Gordon model can simulate the water cycle very well in humid or temperate areas (Gibson, 2002; Gibson et al., 2002, 2006). Because there is an apparent enrichment of the precipitation isotope on the Tibetan Plateau (Tian et al., 2001; Yu et al., 2007), both the equilibrium and the kinetic fractionation processes for calculating the ambient atmospheric vapor isotopes should be considered. It is important to understand the lake water budget and isotope fraction process and its relationship with regional climatic variables at locations such as the alpine arid Tibetan Plateau. The non-equilibrium fraction processes between precipitation and ambient water isotopes are common but primarily influence the water mass balance on the arid western Tibetan Plateau.

The objective of this study was to examine the variation of water $\delta^{18}O$ and *d*-excess in the spatially elongated alpine Lake Bangong (LBG), which is the largest lake in western Tibet, and the correlations of $\delta^{18}O$ and *d*-excess with climatic and environmental factors. In this locality, systematic observation of water isotopes in precipitation, lake water, river water, and groundwater, combined with actual hydrological data and meteorological station data measured in the region of interest, allow for a detailed analysis of the water cycle to promote a further understanding of processes that affect isotopic variation and climate drivers on the arid western Tibetan Plateau. This paper is organized as follows: (1) an investigation of the temporal and spatial variation of $\delta^{18}O$ in lake water and precipitation, river water, and groundwater in the LBG region; (2) the deduction of the E/I ratio of LBG via a modified isotopic enrichment model based on the $\delta^{18}O$ and *d*-excess; and (3) a discussion of the potential relationships between the E/I ratio based on both observed and modeled $\delta^{18}O$ and *d*-excess in lake water. This study is the first comprehensive lake water isotope and geochemical investigation of a large alpine freshwater lake on the arid western Tibetan Plateau.

Regional Setting

Geomorphology

The alpine LBG, located in the arid western Tibetan Plateau between 78°30′–80°E and 33°30′–33°45′N, has a spatially elongated configuration and is the largest lake (604 km^2) in arid western Tibet. Approximately two-thirds (413 km^2) of the lake is in Chinese territory, and the rest is in Indian-controlled Kashmir (Fig. 1). The origin of the lake is attributed to tectonics (Huang et al., 1989), or to a moraine dam at the downstream end of the lake. LBG is a chain of five basins separated by shallow

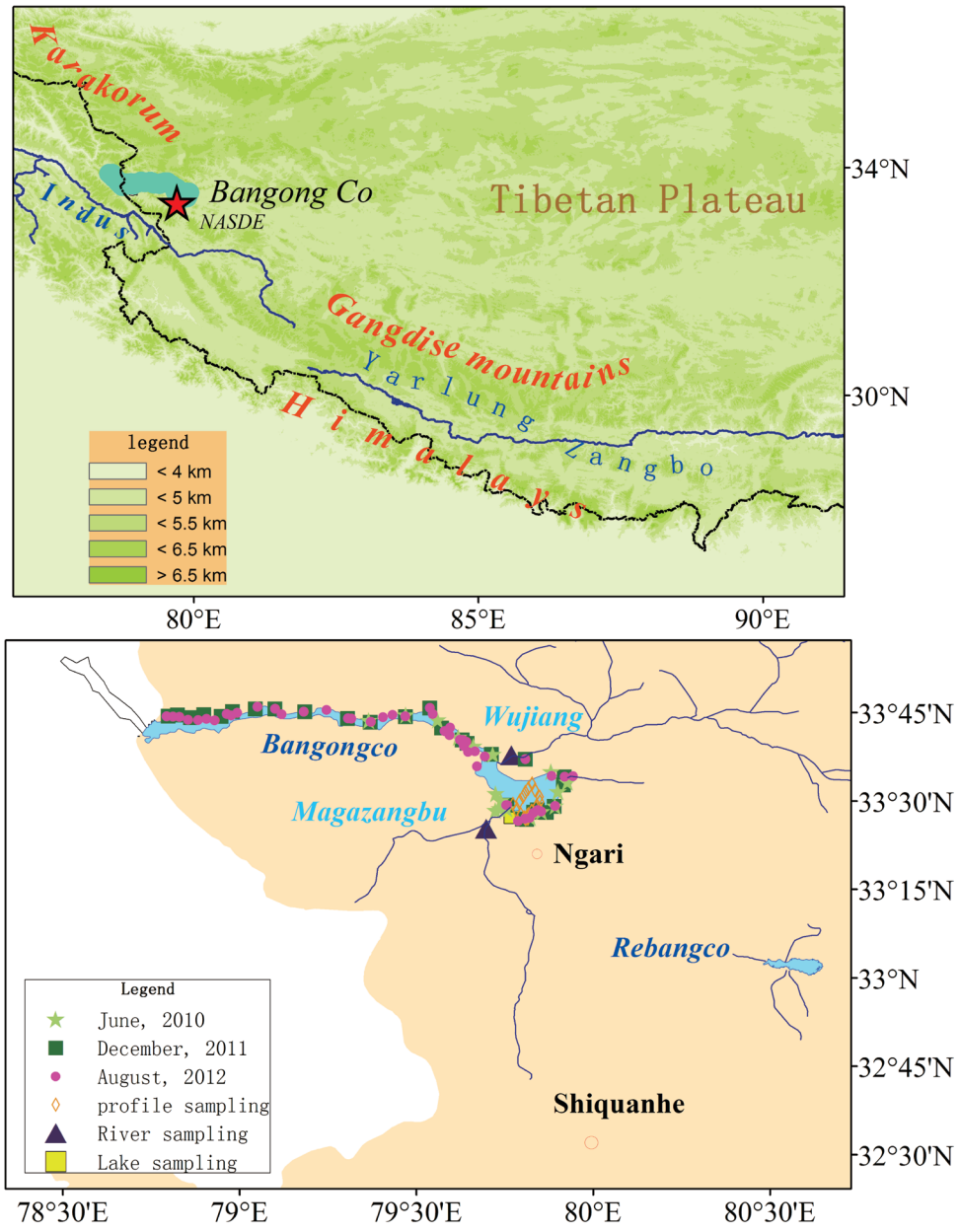

FIGURE 1. Location of the long alpine lake Bangong (LBG) and the water sampling sites, including precipitation, lake, river, subterranean lake profile water sampling, and three periodical spatial lake sampling sites. The yellow solid square indicates the long-term lake sampling site, the purple solid triangles are river sampling sites, the open orange diamonds are the vertical lake profile sampling sites, the light green five-pointed star, the green square, and the pink solid circles indicate the years in which the spatial lake water was sampled (2010, 2011, and 2012, respectively).

sills (Ou, 1981), which thus evolved as a series of individual lakes connected by rivers. The length of the lake is approximately 150 km from east to west, with the width varying from several kilometers in the east to less than 0.1 km in the west. Measurements in the eastern part of the lake indicate that the maximum depth is 43 m (Wang Junbo, personal communication).

Hydrology

LBG is principally supplied by surface runoff flowing into the easternmost sector of the basin. In summer, the ambient lake surface temperature is about 13.3 °C (diurnal observations), which is close to the mean summer surface water temperature of 13.5 °C in central Tibet (Liu et al., 2009). Two principal streams flow into the eastern portion of the lake: the Magazangbu River in the south, which receives mainly local precipitation, and the Wujiang River in the north, which receives water from precipitation as well as from a small amount of glacier melting from a large, glaciated area in the upper basin (Yang et al., 2003).

The nearby Rebang Co is in approximate hydrologic and isotopic steady state and is used to support

the applicability of the steady state model. The annual precipitation amount of the Rebang Co is 50~70 mm and the annual average temperature is 0.0 °C, and it shares the same arid environment as the LBG.

Climate

Arid western Tibet is a cold and windy desert that lies in the rain shadow of the Kunlun and Karakorum mountain ranges. This region is within the extreme range of the Indian monsoon and is mainly influenced by westerlies. Precipitation is concentrated over this region during June to September as either regional rainfall or as rare monsoon rainfall. Automated Weather Station (AWS) observations from the nearby Nagri Station (33.39°N, 79.70°E, 4260 m a.s.l.) show that mean air temperature was 7.4 °C from May to October 2011. The observed total precipitation amount over a two-year period was 180.3 mm, with a large annual variation of 134.4 mm (2010) and 45.9 mm (2011). However, the annual potential evaporation can be as high as 2465.3 mm. The climate conditions are similar to those at the nearby Shiquanhe meteorological station (80.08°N, 32.50°E, 4278 m), which support the soundness of our data.

Materials and Methods

Water Sampling, Measurement, and Lake Water Level Monitoring

Samples from precipitation, streams, and lake water were collected continually during a two-year period from October 2009 to December 2011. Information on sampling locations and frequency is summarized in Table 1. A total of 50 daily precipitation events was collected during the period from October 2009 to December 2011 at Ngari Station. Specially designed bottles, as suggested by the International Atomic Energy Agency (IAEA), were used in the sampling process to minimize the effects of re-evaporation on isotopes. Two collection containers were used in turn; one was used for sampling while the other was drying. The samples were collected daily at 20:00 local time if there was rainfall. Samples of solid precipitation were put into plastic bags, then into plastic bottles after thorough melting at room temperature.

River water was collected weekly from the Magazangbu and Wujiang Rivers; 105 samples were collected from the Magazangbu from October 2009 to December 2011, and 50 were collected from the Wujiang throughout 2011. In addition, 43 weekly underground water samples were collected in 2011 from an existing well with a depth of about 2.5 m.

Lake water was sampled by two methods. The first, in situ sampling, was performed at a fixed site about 5 cm beneath the surface water for temporal lake water isotope change (Fig. 1), with 44 weekly samples collected from 21 December 2011 to 7 November 2012. The second method was spatial sampling along the lake from east to west, which was performed three times over different seasons. The first round of sampling was on 28 June 2010, when 17 samples were collected. The second round of sampling was on 24 December 2011, when 19 samples were collected. On the

TABLE 1

Summary of sampling and isotope values (±1σ) for precipitation, underground water, and lake water in situ sampling and vertical lake water sampling at long alpine lake Bangong (LBG) Basin from 2009 to 2011

Sample types	Station	Longitude	Latitude	Sampling period (yyyy.mm)	No.	$\delta^{18}O$(‰)	δD(‰)	*d*-excess
Daily precipitation	Ngari	79.7°E	33.39°N	2009.10–2011.12	50	–15.62 (±6.2)	–125.80 (±50.0)	–0.85 (±11.0)
Weekly river	Magazangbu	79.7°E	33.39°N	2009.11–2010.9	42			
Weekly river	Magazangbu	79.7°E	33.39°N	2010.10–2011.12	63	–12.23 (±1.5)	–95.13 (±9.0)	1.62 (±4.7)
Weekly river	Wujiang	79.8°E	33.62°N	2010.10–2011.12	50	–12.52 (±0.6)	–94.04 (±2.5)	6.13 (±2.7)
Weekly underground water	Ngari	79.7°E	33.39°N	2011.3–2011.12	43	–12.88 (±0.48)	–96.16 (±1.4)	6.88 (±2.5)
Weekly lake	Bangong	79.8°E	33.44°N	2011.12–2012.11	49	–3.64 (±0.16)	–46.75 (±0.7)	–17.62 (±0.9)

third occasion, we went out on the lake by boat to collect samples from the lake interior on 24 August 2012 and collected 40 samples. These samples were collected near the lake bank by throwing an empty bottle attached to a cord into the lake to minimize the enhanced evaporation of lake water near shore. In addition, nearly 105 vertical lake water samples were sampled at the east opening area of the LBG, with the deepest of the samples at more than 40 m.

All water samples were analyzed using a Picarro L2120-i Liquid Water Analyzer with a precision of ±0.15‰ for $\delta^{18}O$ and ±0.6‰ for δD at the Key Laboratory of Tibetan Plateau Environment Changes and Land Surface Processes (ITPCAS). The isotopic ratio was expressed as per mil relative to the Vienna Standard Mean Ocean Water (VSMOW2) value.

Variations in lake water level and water temperature were measured using a HOBO water level logger, which recorded data hourly from 23 December 2011 to 8 December 2012. The AWS at Ngari Station provided daily meteorological data, including air temperature, relative humidity, and precipitation.

Isotope Fraction Model Description

Lake water isotopes represent a balance between inflow water isotopes and isotope fractionation via surface water evaporation, including both equilibrium fractionation and kinetic fractionation. This variation in isotopic profiles can be simulated using the Rayleigh isotope fractionation model for a closed basin system (Gibson, 2002; Gibson et al., 2002). Here, we used this model to simulate the spatial shift of lake water $\delta^{18}O$ and δD by assuming a different evaporation ratio compared with the total river water inflow into LBG.

For the lake water isotopic budget, we used

$$dV/dt = I - Q - E \tag{1}$$

and

$$V\frac{d\delta_L}{dt} + \delta_L\frac{dv}{dt} = I\delta_I - Q\delta_Q - E\delta_E \tag{2}$$

where V is lake volume, t is time, dV is change in volume over the time interval dt, I is total inflow where $I = I_S + P$ (I_S is surface inflow and P is precipitation on the lake surface), E is evaporation, and δ_L, δ_I, δ_E are the isotopic compositions of lake, inflow, and evaporation flux, respectively.

Lake evaporation is mainly affected by temperature, wind speed, and relative humidity. Craig and Gordon (Craig and Gordon, 1965; Merlivat and Jouzel, 1979) described the isotopic composition of the evaporation flux, δ_E, which can be calculated by

$$\delta_E = (\alpha^*\delta_L - h\delta_A - \varepsilon)/(1 - h + 10^{-3}\varepsilon_K) \tag{3}$$

where $a^\star$ is the equilibrium liquid-vapor isotope fractionation factor as a function of temperature. But these factors are fairly well constrained by laboratory experiments in the range of 0–350 °C, and give experimental values of

$$a^*\left(\frac{18}{}O\right) = Exp\left(-0.002067 - \frac{0.4156}{T} + \frac{1137}{T*T}\right) \tag{4}$$

and

$$a^*\left(\frac{2}{}H\right) = Exp\left(0.05261 - \frac{76.248}{T} + \frac{24844}{T*T}\right) \tag{5}$$

for oxygen-18 and deuterium, respectively, where T is interface temperature (K), h is the relative humidity, and d_A is the isotopic composition of the ambient moisture. ε is the total isotopic separation factor, which is comprised of both equilibrium e^* and kinetic ε_K components, as follows:

$$\varepsilon = \varepsilon^* + \varepsilon_K \tag{6}$$

Equilibrium e^* principally relies on temperature, and kinetic fractionation ε_K is mainly based on relative humidity. e^* is related to $(a^* - 1)$ * 1000. An empirical relationship is used in practice to

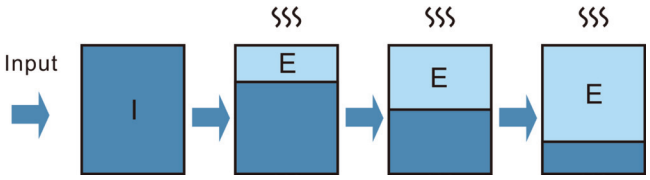

FIGURE 2. A simple schema of a gradual evaporation (E) model from east to west for the LBG.

calculate ε_K (Merlivat, 1978; Merlivat and Jouzel, 1979), as follows:

$$\varepsilon_K\left(\frac{18}{}O\right) = 14.3(1-h) \tag{7}$$

$$\varepsilon_K\left(\frac{2}{}H\right) = 12.5(1-h) \tag{8}$$

We used a partly mixed model to simulate the gradual evaporation in LBG as shown in Figure 2. In this model, the assumed lake water volume does not change as a unit, but there is gradual water flow and gradual evaporation from east to west in the lake. We divided the lake into small box-shaped areas from east to west and assumed that the isotopes of the water were well mixed in each area. We also assumed that the lake water in each area constituted a through-flow body of water. After partial evaporation, the residual water from each box proceeds to the next area, where evaporation occurs in the succeeding box, and the lake water isotopes are thereby enriched.

We then calculated the lake water $\delta^{18}O$ and δD for this model using a twofold isotope fractionation process. First, we treated each box-shaped area as a through-flow water body by introducing a through-flow index, x, representing the fraction of evaporation to water inflow (Gibson et al., 2002). This allows for a simulation of the residual water $\delta^{18}O$, δD in each box-shaped area. Next, we simulated the gradual $\delta^{18}O$, δD enrichment from the first box to subsequent box-shaped areas. In this process, we simulated the water $\delta^{18}O$, δD in the first box by assuming that the water body isotopic content was the same as the initial river water $\delta^{18}O$, δD. A minor portion of lake water δV evaporated from the water surface with an evaporating isotope composition of δE. The residual lake water will be slightly enriched in heavy isotopes to a value of δ_{L1},

$$\delta_{L1} = \frac{V\delta_o - \Delta V\delta_E}{V - \Delta V} \tag{9}$$

Then, we assumed a small portion of inflow water δ_V with δ_I and that the lake water will maintain the same volume V but that the lake water isotope composition will change to δ_{L2},

$$\delta_{L2} = \frac{(V - \Delta V)\delta_{L1} + \Delta V\delta_I}{V} \tag{10}$$

Each step will take a time $\tau\delta V/V$, where τ is the residence time of water in a steady state lake, which is given as

$$\tau = \frac{V}{I} \tag{11}$$

With the subsequent repeated steps of lake water evaporation and inflow water replenishment, the model can simulate the progressive enrichment in the heavy isotopes in lake water with time within each box. The lake water isotope composition will attain a constant value of δ_S. We also assumed the lake water is well mixed after each step within each box. The simulated constant $\delta^{18}O$, δD of the first box residual water was set as the inflow of water isotopes for the next box. As the above process continues, the residual lake water in the subsequent box-shaped areas become enriched with the increasing E/I ratio.

Under mean annual conditions, the d_A of atmospheric moisture is assumed to be close to equilibrium with the stable isotope of precipitation, as found in many other studies (Craig and Gordon, 1965; Gibson et al., 2016). There is an increasing trend of water isotopes, including precipitation and water vapor from south to north on the Tibetan Plateau, which is significantly different from the "continental effect." This non-equilibrium between precipitation and lake water isotopes should be considered when modeling the isotope fractionation of lake wa-

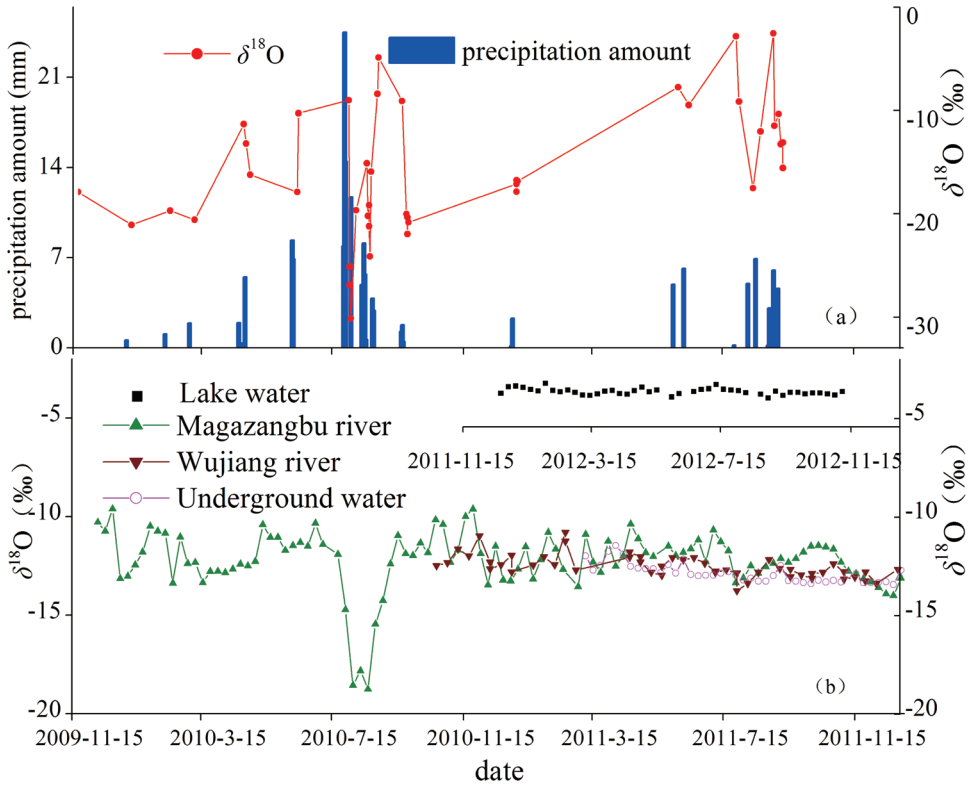

FIGURE 3. Temporal variation in the water $\delta^{18}O$ in the LBG Basin, for (a) daily precipitation $\delta^{18}O$ and precipitation amounts at the Ngari Station 2009–2011, (b) for weekly river $\delta^{18}O$ in the Wujiang in 2011, the Magazangbu 2010–2011, and weekly groundwater $\delta^{18}O$ at Ngari Station; and weekly lake $\delta^{18}O$ in 2011–2012.

ter in northern arid regions. Thus, a fully kinetic fraction involved evaporation assumption between precipitation and ambient vapor isotopes has been applied to approximate the value of d_A ($\delta_A = \delta_P - \varepsilon^* - \varepsilon_K$).

Results and Discussion

Temporal Variation of $\delta^{18}O$ in Precipitation, River, and Lake Water in the LBG Basin

In the LBG Basin, the isotopic composition was found to be lighter in precipitation than in river and lake water (Table 1). The mean $\delta^{18}O$ in precipitation was –15.62‰, with a standard deviation (±1s) of 6.2‰. The mean δD in precipitation was –125.80‰, with a standard deviation of ±50.0‰. The mean isotopic values from LBG were very close to those for the Magazangbu and Wujiang Rivers, with –12.23‰ (with a standard deviation of ±1.5‰), –12.52‰ (with a standard deviation of ±0.6‰) for $\delta^{18}O$, respectively, and –12.88‰ for ground water (with a standard deviation of ±0.48‰), indicating a single water source. The observed isotopic composition of the lake water was significantly enriched, with –3.64‰ (with a standard deviation of ±0.16‰) for $\delta^{18}O$.

The $\delta^{18}O$ of precipitation varied significantly from –30.11‰ to –2.55‰ over the seasons (Fig. 3; Table 1). The large fluctuations in the precipitation $\delta^{18}O$ are partly due to the effect of summer monsoon precipitation. During the encroachment of the Indian monsoon between 26 and 29 July 2010, the $\delta^{18}O$ in precipitation rapidly decreased from –9.0‰ to –30.11‰, while the extreme precipitation amount was more than 25 mm (Fig. 3, part a). Variation of river water $\delta^{18}O$ was more stable when compared to that of precipitation (Fig. 3, part b). However, seasonal variation of precipitation affects the isotopic composition of stream water. The extreme precipitation event led to the sharp drop of $\delta^{18}O$ in both precipitation and river water. The $\delta^{18}O$ in the Magazangbu fell to a minimum of –18.55‰ from 26 to 28 July 2010 (Fig. 3, part a).

The results from weekly lake water sampling showed that the lake $\delta^{18}O$ was almost stable, especially when the value was compared to the variations of precipitation and river water (Fig. 3, part b). The seasonal lake water level changed within only 20 cm, a

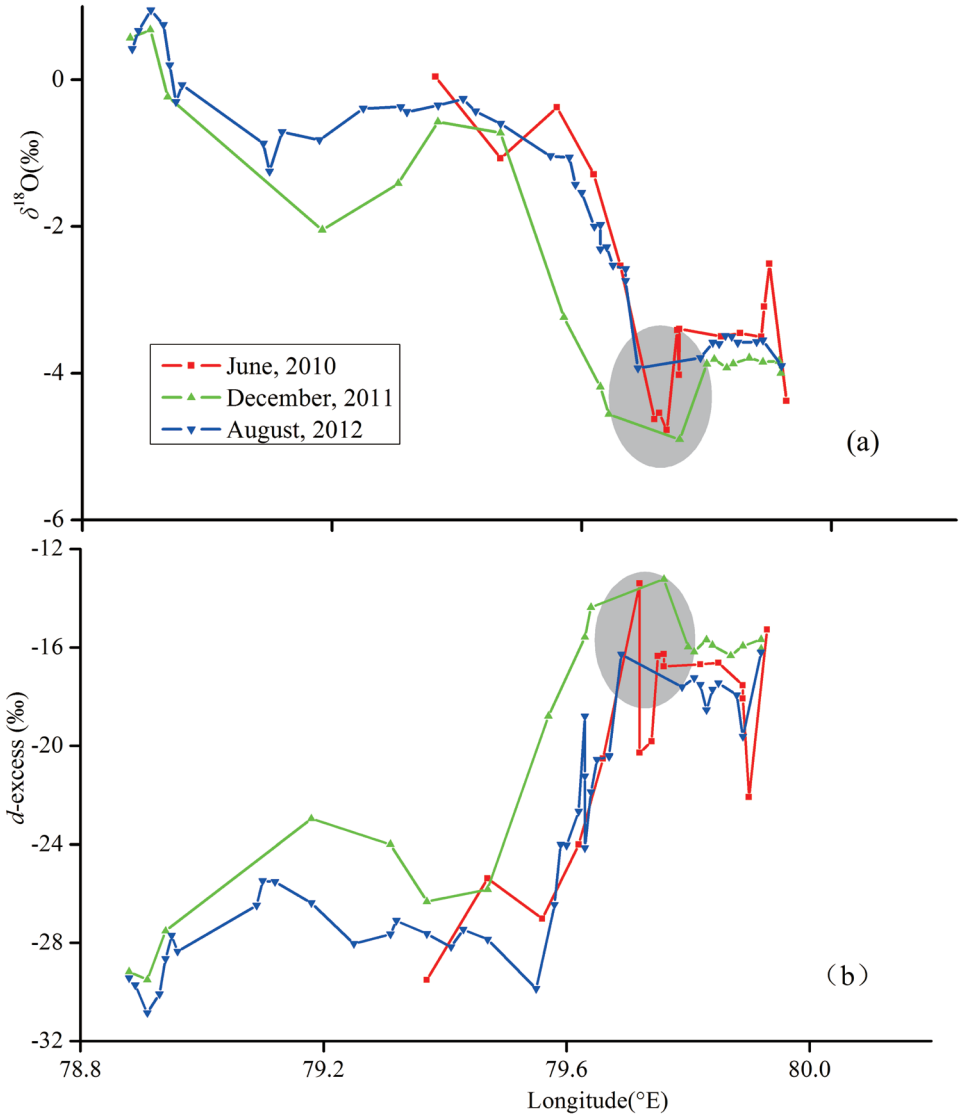

FIGURE 4. Longitudinal variations in LBG lake water (a) $\delta^{18}O$ and (b) *d*-excess based on three field observations: June 2010 (red line), December 2011 (green line), and August 2012 (blue line). The shaded area shows the direct contribution of the input water from the Magazangbu River.

result related to lower precipitation in the catchment in winter. This result validated the assumption of a constant lake water volume in the isotope model.

Longitudinal Variations of Lake $\delta^{18}O$ and *d*-Excess

Figure 4, part a, shows the longitudinal $\delta^{18}O$ and *d*-excess variation for lake water. There is a robust increasing trend in lake $\delta^{18}O$ from east to west. The roughly seasonal consistency in spatial lake $\delta^{18}O$ implies that the observed trends are representative and persistent. $\delta^{18}O$ in lake water varied within a range from –2.51‰ to –4.90‰ in the eastern, open water area between 79.7°E and 80.0°E. Westward, $\delta^{18}O$ in lake water increased to –1.59‰ from 79.7°E to 79.0°E. As the evaporation process continued, the value of $\delta^{18}O$ kept rising from the open water area of the east to the west. In the westernmost part of the lake, $\delta^{18}O$ in lake water increased to slightly above 0.36‰.

The spatial variation of lake water *d*-excess showed a divergence opposite to the $\delta^{18}O$ changes (Fig. 4, part b). The *d*-excess was about –17.0‰ in the eastern, open water area between 79.7°E and 80.0°E, –23.97‰ from 79.7°E to 79.0°E, and had an extremely negative value of –29.10‰ in the westernmost sector.

Lake $\delta^{18}O$ in December 2011 was consistently lower than in summer over longitudinal transects, while the *d*-excess was significantly higher. This may be because most of the lake surface was covered by ice, which effectively prevented lake sur-

face evaporation. A slight variation in $\delta^{18}O$ in the eastern part of the lake is related to the location of river water input and its distance to the river mouth. An exceptionally low $\delta^{18}O$ near 79.7°E is related to the direct contribution of the input water from the Magazangbu River (the shaded area in Fig. 4, part a).

Simulated Results

As a first step, a simple steady-state model (Gibson et al., 2002) was used to test the simulation's capacity for capturing the lake isotope signal. The lake water was assumed to be isotopically mixed with a constant volume. The observed precipitation and river $\delta^{18}O$, δD were used as the inflow water isotope value and combined with the meteorological data. The final simulated mixed closed lake water reached a constant value through the full kinetic isotope fractionation process of atmospheric water vapor, with –1.0‰ for $\delta^{18}O$, and –31.2‰ for *d*-excess, respectively (Fig. 5). We first evaluated the reliability of the model by simulating the lake $\delta^{18}O$ and *d*-excess in the nearby lake, Rebang Co. This simulated result is in close agreement with the observed lake water of 0.21‰ for $\delta^{18}O$, and –29.4‰ for *d*-excess (Fig. 1). This agreement validates this application of the steady-state isotope model. With average relative humidity of about 54%–58% at the Yamdruk-tso basin on the southern Tibetan Plateau (Tian et al., 2008), it is reasonable to assume that relative humidity is about 35% from the Ngari meteorological data and corresponds to the modeled present $\delta^{18}O$ value of lake water at the steady state of LBG on the far western arid Tibetan Plateau.

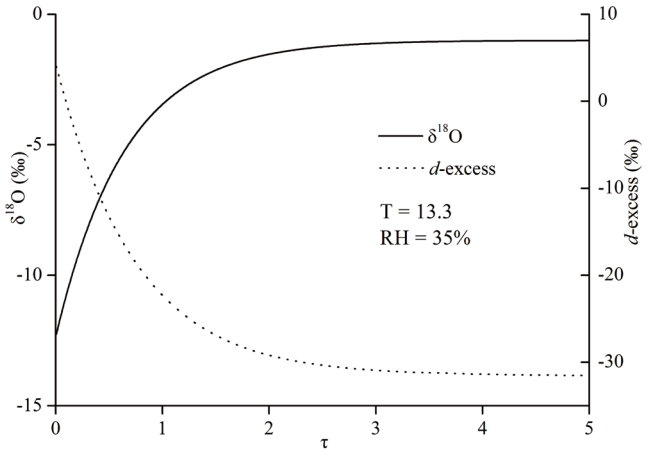

FIGURE 5. The model simulation of closed lake $\delta^{18}O$ (solid line) and *d*-excess (dashed line) in lake water over time for the assumed steady state. The abscissa is for time expressed in τ, the residual time of water in a lake.

The model results show that, with lake water evaporation and inflow to the lake, the $\delta^{18}O$ of the residual lake water will rise and the *d*-excess of the residual lake water will decrease due to the isotopic fractionation in the evaporation process and will eventually reach a constant value. The change of both the lake $\delta^{18}O$ and *d*-excess at the beginning stage is so fast that even assuming a very low initial lake water temperature or relative humidity, the time to reach isotopic steady state is not increased. However, the following lake water isotope equilibrium may take a rather long time to reach the absolute constant values.

Therefore, we used a modified, partly mixed isotope model to simulate progressive changes in the lake water. The lake water $\delta^{18}O$ (or δD) observed in different parts of LBG can be transferred to specific E/I ratios. Initially observed input data are listed in Table 2. The precipitation input for the lake surface has been ignored; we assume the inflow isotope because the lake surface is relatively small compared to the catchment area (approximately 1.4%). We assume that the initial lake water is the same as the average of river water, with $\delta^{18}O$ of –12.35‰ and δD of –94.55‰, which was the average measured value for the inflow river (Table 2). Precipitation isotopes are used here to calculate the value of ambient vapor. With this modified partly mixed model, the simulated response of LBG water $\delta^{18}O$ (or δD) to different E/I ratios under present hydrometeorological conditions is presented in Figure 6.

The modeling results show that the $\delta^{18}O$ of –3.6‰ and *d*-excess of –17.6‰ correspond to an E/I ratio of approximately 0.79 at the fixed lake water sampling position in the eastern lake. This result means that 79% of the input water had evaporated. The model was focused on simulated results for LBG water $\delta^{18}O$ over a range of –5.0‰ to +0.95‰, and *d*-excess over a range of –30.9‰ to –13.2‰. We modeled both the lake $\delta^{18}O$ (Fig. 6, part a) and *d*-excess (Fig. 6, part b) that correspond to the E/I ratios from east to west. The simulated E/I ratios from both $\delta^{18}O$ and *d*-excess of lake water are consistent with each other. For

TABLE 2

Initial data for the stable isotope fractionation model.

Data	Parameter	Measurement	Data source
Hydrometeorological	T_{water}	13.3 °C	Water level gauge (2011.05–2011.10)
	T_{air}	7.4 °C	Automatic meteorological station (2011.05–2011.10)
	RH	35%	
Water isotopes	δ_I for $\delta^{18}O$	–12.35‰	This study
	δ_I for δD	–94.55‰	This study
	δ_P for $\delta^{18}O$	–15.62‰	This study
	δ_P for δD	–125.80‰	This study
	δ_L for $\delta^{18}O$	–3.64‰	This study
	δ_L for δD	–46.75‰	This study

Time given as yyyy.mm.

the observed –4.9‰ of $\delta^{18}O$, –13.2‰ of *d*-excess for the lake water at the easternmost site, the E/I ratio is approximately 0.73, while in the westernmost position, the +0.95‰ of $\delta^{18}O$, –30.9‰ of *d*-excess for the lake corresponds to an E/I ratio of 0.93. The relationship between the E/I ratio and the simulated lake $\delta^{18}O$ or lake *d*-excess showed a good fit.

In addition, the relationships between $\delta^{18}O$ and δD are built to verify the simulation results based on the observed data and simulation data (Fig. 7). The line regression is $\delta D = 5.00 * \delta^{18}O - 28.48$ ($R^2 = 0.98$) based on field isotope data, which is close to the model simulation regression line, $\delta D = 4.57 * \delta^{18}O - 28.06$ ($R^2 = 1$). The variations of lake isotopes and E/I ratio can properly simulate and represent the lake water cycle of alpine LBG on the western Tibetan Plateau.

Sensitivity Test

Various parameters affect the lake water cycle process in the isotope fractionation model. To evaluate the contribution of different parameters, sensitivity tests for various climatic parameters, including both relative humidity levels (Fig. 8, parts a and b) and lake water temperatures (Fig. 8, parts c and d), and the initial inflow of the isotope values (Fig. 8, parts e and f) were performed. The model results show that the E/I ratio that corresponds to lake $\delta^{18}O$ level is very much dependent on relative humidity rather than lake water temperature (Fig. 8, parts a and c). Lower relative humidity, lower lake water temperature, and

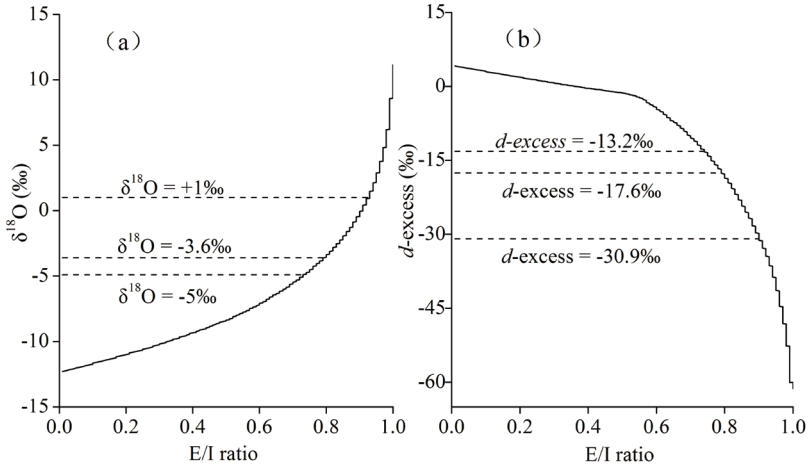

FIGURE 6. Simulated variation of lake water (a) $\delta^{18}O$ and (b) *d*-excess evolution processes in the LBG with increasing E/I ratios under present hydrometeorological conditions. The values of lake $\delta^{18}O$ and *d*-excess at three sites were selected and marked on the graph: (1) at the easternmost site with a value of –5.0‰ for $\delta^{18}O$ and –13.2‰ for *d*-excess, (2) at the fixed sampling site with a value of –3.6‰ for $\delta^{18}O$ and –17.6‰ for *d*-excess, and (3) at the westernmost site with a value of +1.0‰ for $\delta^{18}O$ and –30.9‰ for *d*-excess.

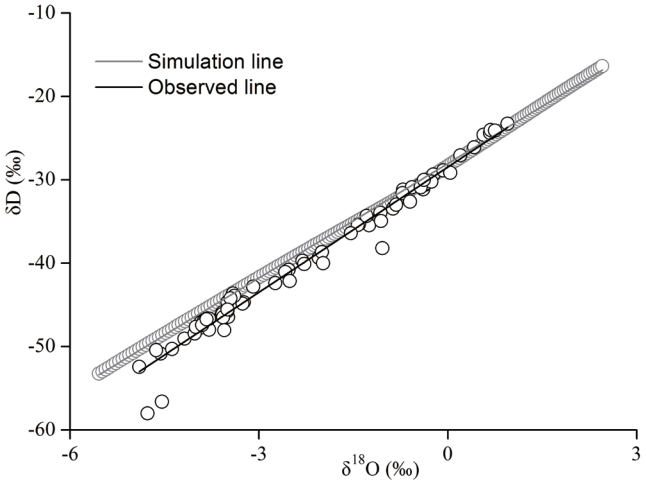

FIGURE 7. Relationship between $\delta^{18}O$ and δD of the lake water isotopes based on field observation data (black circles) and model simulation results (gray circles). The regression line of the observed line is $\delta D = 5.00 * \delta^{18}O - 28.48$ ($R^2 = 0.98$). The regression line of the simulation line is $\delta D = 4.57 * \delta^{18}O - 28.06$ ($R^2 = 1$).

strong evaporation will lead to a more enriched $\delta^{18}O$ value. The model results imply that local relative humidity is a crucial factor that influences the evaporation process of lake water.

The impact of regional climatic parameters on the evolution of lake *d*-excess as they correspond to E/I ratio was also tested (Fig. 8, parts b and d). Both relative humidity and lake temperature significantly influence lake *d*-excess. The simulated final lake water *d*-excess is more negative under lower relative humidity and higher lake water temperature. As the evaporation process continues, the lake $\delta^{18}O$ gets more enriched, while the lake *d*-excess gets more depleted under different climatic parameters. These results agree with the evolution of isotopic evaporation in lake water in other regions, where relative humidity is the essential factor controlling the inland arid alpine lake water (Gat and Airey, 2006; Tian et al., 2008; Gao et al., 2009). We also noticed that the background meteorological conditions were not useful for running this fully kinetic model when relative humidity values were too high. The variation of both $\delta^{18}O$ and *d*-excess becomes indistinct when the humidity value reaches about 60% (Fig. 8, part a and c). This modified partly mixed model only fit for the far western arid alpine region.

To evaluate the influence of different distributions of precipitation and river water budgets, we modeled the lake water $\delta^{18}O$ and *d*-excess changes by assuming different percentages of precipitation and river inflow in present climate conditions (Fig. 8, parts e and f). We summarize the evolution process of the lake water isotopes under various values of initial inflow, mainly from three periods, that is, I_R accounting for 100% stage; I_R, I_P accounting for 50%, respectively; I_P accounting for 100%. Results show that there is no big discrepancy in the initial isotope values for full precipitation and river water. This result implies that the lake E/I is not sensitive to the change of the inflow $\delta^{18}O$ and *d*-excess variation.

Implications of Water Cycle and Climate Change for the Alpine LBG

Notable spatial variations of LBG $\delta^{18}O$ and *d*-excess can be interpolated as spatial E/I ratios for different parts of the lake from east to west with inverse distance interpolation (IDW) (Fig. 9). The spatial change in the E/I ratios allows for analysis of the in-lake water cycle. In the extreme eastern open water zone, ~0.73–0.83 of the inflow water evaporates to the atmosphere. The E/I ratio increases to ~0.75–0.90 in the central LBG, and up to ~0.90–0.93 in the westernmost part. This increased E/I represents a cumulative evaporative enrichment effect, which shows that the distinctive in-lake water cycle leads to the spatial variation of E/I.

Some uncertainties may affect the simulated results. Considering the representative nature of the lake samples, spatial lake water was sampled three times in different seasons to limit the possible effects of seasonality. The depth profile of the lake was sampled from the lake interior to decrease the impact of possible evaporation at or near the shallow bank area. However, the sampling coverage was still quite limited relative to the entire, large lake surface area, especially in the open water area in the east. Therefore, the results can give only a rough quantitative estimation of the longitudinal trend of the E/I ratio in different parts of the lake. Moreover, some small rivers flow into the western part of the lake and thus slightly lower the lake $\delta^{18}O$ value. In several earlier studies, the ambient vapor is assumed to be in equilibrium with the annual precipitation isotopes (Gibson, 2002; Gibson et al., 2016). However, the inland region is significantly affected by local water recycling due to

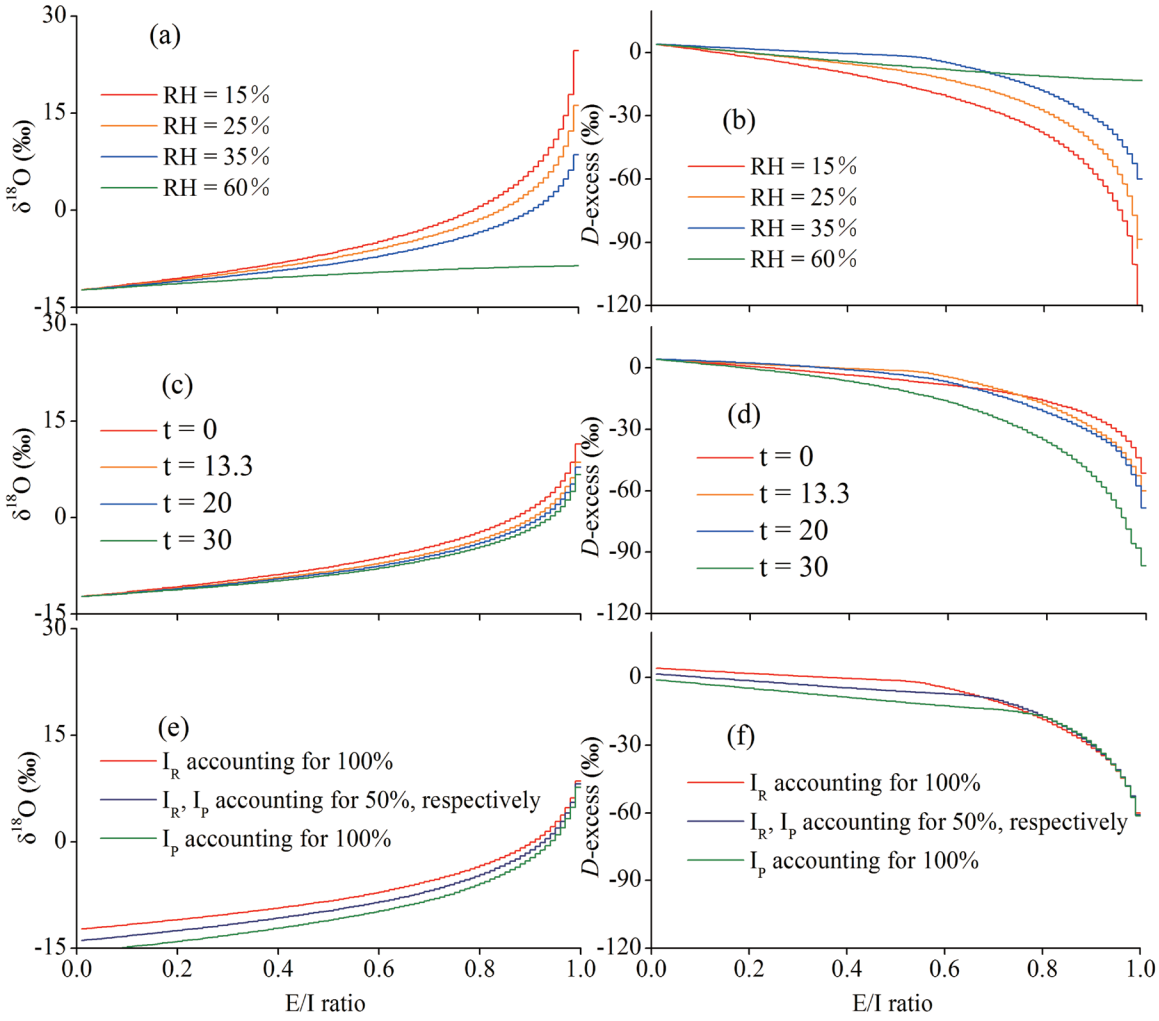

FIGURE 8. Simulated (a) $\delta^{18}O$ and (b) *d*-excess evolution response to E/I ratio in the LBG, assuming various relative humidity levels; for lake water temperatures (c and d); and for initial inflow isotope value (e and f), respectively.

an increasingly arid climate toward the northern plateau. This causes a trend of enrichment of the precipitation isotope (Tian et al., 2001), and non-equilibrium between precipitation and ambient vapor isotope as well. If this kinetic effect between precipitation and vapor isotopes is not considered, there will be a failure in rebuilding the observed spatial change of both lake $\delta^{18}O$ and *d*-excess. In our model, we use a full kinetic isotope fractionation model to capture the measured Bangong Co lake water $\delta^{18}O$ and *d*-excess, reconfirming the strong local water cycling in the arid region of the western Tibetan Plateau. Our research also shows the importance of observed ambient vapor in the lake water isotope simulation. Unfortunately, no directly measured long-term ambient vapor isotope data are currently available, but we will try to measure these data in the future.

Because most of the lakes on the arid western Tibetan Plateau are located in remote regions where physical access is difficult, major knowledge gaps exist in the behavior of the region's hydrological and water resources. Water isotopes provide a practical method to monitor the water inflow processes. Because most of the input water comes from eastern rivers, the actual inflow from east to west inside the lake can be determined from the spatial salinity and the isotopes in the lake water. Because of the uneven distribution of river mouths in most of the Tibetan lakes, an understanding of the inland lake water cycle becomes important and necessary. Apparent spatial

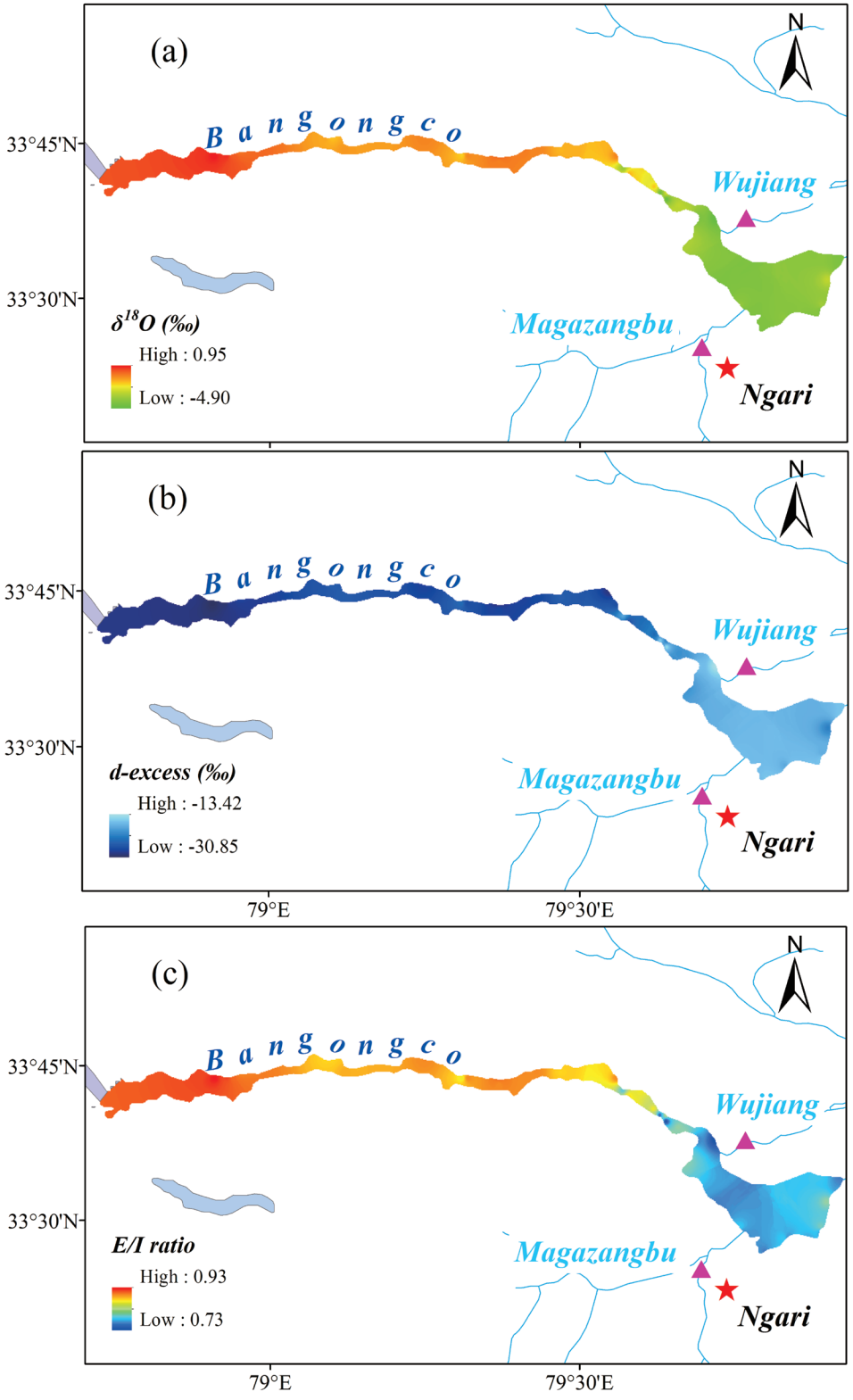

FIGURE 9. Estimation of spatial variations for the LBG for (a) lake $\delta^{18}O$; (b) lake *d*-excess, and (c) calculated E/I ratio.

variations in the lake water $\delta^{18}O$ and E/I ratios may be related to the variability of climate and hydrological conditions. This analysis may suggest topics for further research on lake isotopes. A large water budget shift on the Tibetan Plateau in the coming years will certainly change lake water isotopes (Lei et al., 2014; Zhang et al., 2013, 2014). The water $\delta^{18}O$ signature in the vast number of lakes across the inner Tibetan Plateau is likely to be inconsistent. Therefore, such studies may aid in

understanding the various patterns of climate evolution and hydrological conditions on the Tibetan Plateau.

The expansion or shrinkage of a lake changes the distance to the mouth of the river, and thus the E/I ratio, for a large lake. Various factors affect the isotope record, including the local climate, changes in atmospheric circulation, and the residual time (Fontes et al., 1996), making an explicit interpretation of the isotope record difficult. In addition, the means by which the modern regional water cycle and the hydrological process can change the lake sediment isotope record is not quantitatively understood. In this sense, our study can facilitate the interpretation of the isotope record from lake sediments on the Tibetan Plateau in the future.

Conclusions

Application of the isotope technique provides a useful tool for understanding the hydrological cycle in an inland basin. Lake water isotope variation can reflect the local water cycle in the catchment as well as in the inflow process, owing to climate changes, especially on the arid western Tibetan Plateau. Over two years of continual observation of water isotopes in the alpine LBG catchment allowed for a simulation of the lake isotope and the lake water cycle. The lake $\delta^{18}O$ is approximately –3.64‰ at the fixed sampling site in the eastern open water, which is >10‰ higher than the local precipitation, with the $\delta^{18}O$ of –15.62‰. The large difference reflects the strong evaporation enrichment of the heavy isotopes in the steady lake system. Data from three different periods of spatial sampling along the alpine LBG show that the spatial variation of lake $\delta^{18}O$ and *d*-excess are apparent, ranging from approximately –4.9‰ to +0.9‰ for $\delta^{18}O$, and –13.22‰ to –30.85‰ for *d*-excess, respectively, from east to west in the lake.

By combining both the $\delta^{18}O$ and δD of the local precipitation and the river water, a modified partly mixed isotope fractionation model can be used to depict the evaporation process of lake water. The simulation results based on the isotope technique show that present lake water $\delta^{18}O$ and δD levels correspond to an average relative humidity of around 35% during evaporation, which is identical to average relative humidity during the evaporation season from local meteorological data. The gradual increase in the E/I ratio was simulated along the LBG from east to west and was most notably influenced by the kinetic fractionation process during the evaporation of the lake. Approximately 0.73–0.83 of the input water was evaporated in the eastern part, while ~0.90–0.93 evaporated in the western part of the alpine LBG. This study's linkage of the spatial variation of the water isotopes with the E/I ratio may provide clues for further determining the evolutionary pattern of lake water on the distant arid western Tibetan Plateau. Also, it potentially could shed light on the interpretation of lake sediments.

Acknowledgments

This research was supported by the National Natural Science Foundation of China (Grant Nos. 91437110 and 41371086) and Chinese Academy of Sciences (Grant No. XDB03030100). We thank Dr. Anne Jennings and two anonymous reviewers for their comments and suggestions.

References Cited

Bowen, G. J., Kennedy, C. D., Liu, Z., and Stalker, J., 2011: Water balance model for mean annual hydrogen and oxygen isotope distributions in surface waters of the contiguous United States. *Journal of Geophysical Research*, 116(G4): G04011, doi http://dx.doi.org/10.1029/2010JG001581.

Brooks, J. R., Gibson, J. J., Birks, S. J., Weber, M. H., Rodecap, K. D., and Stoddard, J. L., 2014: Stable isotope estimates of evaporation : inflow and water residence time for lakes across the United States as a tool for national lake water quality assessments. *Limnology and Oceanography*, 59: 2150–2165.

Craig, H., and Gordon, L. I., 1965: Deuterium and oxygen 18 variations in the ocean and the marine atmosphere. *In* Tongiorgi, E. (eds.), *Stable Isotopes in Oceanographic Studies and Paleotemperatures.* Pisa, Italy: CNR, 9–130.

Dansgaard, W., 1964: Stable isotopes in precipitation. *Tellus*, 4: 436–468.

Fontes, J. C., Gasse, F., and Gibert, E., 1996: Holocene environmental changes in Bangong Co Basin (Western Tibet). Part 1: chronology and stable isotopes of carbonates of a Holocene lacustrine core. *Palaeogeography, Palaeoclimatology, Palaeoecology*, 120: 25–47.

Gao, J., Tian, L. D., Liu, Y. Q., and Gong, T. L., 2009: Oxygen isotope variation in the water cycle of the Yamzho Lake Basin in Southern Tibetan Plateau. *Chinese Science Bulletin*, 54(16): 2758–2765.

Gasse, F., Arnold, M., Fontes, J. C., Fort, M., Gibert, E., Huc, A., Bingyan, L., Yuanfang, L., Qing, L., Melieres, F., Van Campo, E., Wang, F., and Zhang, Q., 1991: A 13,000-year climate record from Western Tibet. *Nature*, 353: 742–745.

Gasse, F., Fontes, J. C., Campo, E. V., and Wei, K., 1996: Holocene environmental changes in Bangong Co Basin (Western Tibet). Part 4: discussion and conclusions. *Palaeogeography, Palaeoclimatology, Palaeoecology*, 120: 72–92.

Gat, J. R., 1996: Oxygen and hydrogen isotopes in the hydrologic cycle. *Annual Review of Earth and Planetary Sciences*, 24: 225–262.

Gat, J. R., and Airey, P. L., 2006: Stable water isotopes in the atmosphere/biosphere/lithosphere interface: scaling-up from the local to continental scale, under humid and dry conditions. *Global and Planetary Change*, 51(1-2): 25–33.

Gibson, J. J., 2002: Short-term evaporation and water budget comparisons in shallow Arctic lakes using non-steady isotope mass. *Journal of Hydrology*, 264: 242–261.

Gibson, J. J., Prepas, E. E., and McEachern, P., 2002: Quantitative comparison of lake throughflow, residency, and cathchment runoff using stable isotopes: modelling and results from a regional survey of boreal lakes. *Journal of Hydrology*, 262: 128–144.

Gibson, J. J., Prowse, T. D., and Peters, D. L., 2006: Hydroclimatic controls on water balance and water level variability in Great Slave Lake. *Hydrological Process*, 20(19): 4155–4172.

Gibson, J. J., Birks, S. J., and Yi, Y., 2016: Stable isotope mass balance of lakes: a contemporary perspective. *Quaternary Science Reviews*, 131: 316–328.

Grafenstein, U., Erlenkeuser, H., Muller, J., Trimborn, P., and Alefs, J., 1996: A 200 year mid-European air temperature record preserved in lake sediments: an extension of the $\delta^{18}O_p$-air temperature relation into the past. *Geochimica et Cosmochimica Acta*, 60(21): 4025–4036.

Huang, C. X., Zhang, Q. S., and Liu, F. T., 1989: A preliminary study of paleovegetation and paleoclimate in the later period of late Pleistocene in Bangongcuo Lake region of Xizang. *Journal of Natural Researches*, 4: 247–253.

Immerzeel, W. W., Van Beek, L. P., and Bierkens, M. F., 2010: Climate change will affect the Asian water towers. *Science*, 328(5984): 1382–1385.

Kropacek, J., Braun, A., Kang, S., Feng, C., Ye, Q., and Hochschild, V., 2012: Analysis of lake level changes in Nam Co in central Tibet utilizing synergistic satellite altimetry and optical imagery. *International Journal of Applied Earth Observation and Geoinformation*, 17: 3–11.

Lei, Y. B., Yang, K., Wang, B., Sheng, Y. W., Bird, B. W., Zhang, G. Q., and Tian, L. D., 2014: Response of inland lake dynamics over the Tibetan Plateau to climate change. *Climatic Change*, 125(2): 281–290.

Liu, Z. F., Tian, L. D., Yao, T. D., and Gong, T. L., 2009: Estimation of evaporation from Cona Lake in the central Tibetan Plateau using an isotope-based method. *Journal of Nature Resource*, 24: 2014–2023.

Lu, A. X., Yao, T. D., Wang, L. H., Liu S. Y., Guo, Z. L., 2005: Study on the fluctuations of typical glaciers and lakes in the Tibetan Plateau using remote sensing. *Journal of Glaciology and Geocryology*, 27(6): 783–792.

Masson-Delmotte, V., Hou, S. G., Ekaykin, A., Jouzel, J., Aristarain, A., Bernardo, R. T., Bromwich, D., Cattani, O., Delmotte, M., Falourd, S., Frezzotti, M., Gallée, H., Genoni, L., Isaksson, E., Landais, A., Helsen, M. M., Hoffmann, G., Lopez, J., Morgan, V., Motoyama, H., Noone, D., Oerter, H., Petit, J. R., Royer, A., Uemura, R., Schmidt, G. A., Schlosser, E., Simões, J. C., Steig, E. J., Stenni, B., Stievenard, M., van den Broeke, M. R., van de Wal, R. S. W., van de Berg, W. J., Vimeux, F., and White, J. W. C., 2008: A review of Antarctic surface snow isotopic composition: observations, atmospheric circulation, and isotopic modeling. *Journal of Climate*, 21(13): 3359–3387.

Merlivat, L., 1978: Molecular diffusivities of $H_2{}^{16}O$, $HD^{16}O$, and $H_2{}^{18}O$ in gases. *Journal of Chemical Physics*, 69(6): 2864–2871.

Merlivat, L., and Jouzel, J., 1979: Global climate interpretation of the deuterium-oxygen 18 relationship for precipitation. *Journal of Geophysical Research*, 84: 5029–5033.

Ou, Y.-X., 1981: Hydrologic characteristics of the east Bangong Lake. *In Geological Xizang (Tibet) Plateau and Ecological Studies of Qinghai-Xizang Plateau*. Beijing: Science Press, 1713–1717.

Song, C., Huang, B., and Ke, L., 2013: Modeling and analysis of lake water storage changes on the Tibetan Plateau using multi-mission satellite data. *Remote Sensing of Environment*, 135: 25–35.

Song, C., Huang, B., Ke, L., and Richards, K. S., 2014: Seasonal and abrupt changes in the water level of closed lakes on the Tibetan Plateau and implications for climate impacts. *Journal of Hydrology*, 514: 131–144.

Tian, L., Masson-Delmotte, V., Stievenard, M., Yao, T., and Jouzel, J., 2001: Tibetan Plateau summer monsoon northward extent revealed by measurements of water stable isotopes. *Journal of Geophysical Research: Atmospheres,* 106: 28081–28088.

Tian, L. D., Liu, Z. F., Gong, T. L., Yin, C. L., Yu, W. S., and Yao, T. D., 2008: Isotopic variation in the lake water balance at the Yamdruk-Tso basin, southern Tibetan Plateau. *Hydrological Processes*, 22(17): 3386–3392.

Wang, R. L., Scarpitta, S. C., Zhang, S. C., and Zheng, M. P., 2002: Later Pleistocene/Holocene climate conditions of Qinghai? Xizhang Plateau (Tibet) based on carbon and oxygen stable isotopes of Zabuye Lake sediments. *Earth and Planetary Science Letters*, 203(1): 461–477.

Wang, S. M., 1998: *An Overview of Lakes over China*. Beijing: Science Press.

Wu, Y. H., Zheng, H. X., Zhang, B., Chen, D. M., and Lei, L. P., 2014: Long-term changes of lake level and water budget in the Nam Co Lake basin, central Tibetan Plateau. *Journal of Hydrometeorology*, 15(3): 1312–1322.

Yang, H. A., Li, Z. Q., Ye, B. S., Jiao, K. Q., 2003: New result of glacier inventory in the drainage basins of the Bangong Lake in China. *Journal of Glaciology and Geocryology*, 25(6): 685–691.

Yao, T. D., Pu, J. C., Lu, A. X., Wang, Y. Q., and Yu, W. S., 2007: Recent glacial retreat and its impact on

hydrological processes on the Tibetan Plateau, China, and surrounding regions. *Arctic, Antarctic, and Alpine Research*, 39(4): 642–650.

Ye, Q. H., Zhu, L. P., Zheng, H. X., Naruse, R., Zhang, X. Q., and Kang, S. C., 2007: Glacier and lake variations in the Yamzhog Yumco basin, southern Tibetan Plateau, from 1980 to 2000 using remote-sensing and GIS technologies. *Journal of Glaciology*, 53(183): 673–676.

Yu, W. S., Yao, T. D., Tian, L. D., Ma, Y. M., Kurita, N., Ichiyanagi, K., Wang, Y., and Sun, W. Z., 2007: Stable isotope variations in precipitation and moisture trajectories on the western Tibetan Plateau, China. *Arctic, Antarctic, and Alpine Research*, 39(4): 688–693.

Yu, W. S., Ma, Y. M., Sun, W. Z., and Wang, Y., 2009: Climatic significance of $\delta^{18}O$ records from precipitation on the western Tibetan Plateau. *Chinese Science Bulletin*, 54(16): 2732–2741.

Yuan, F. S., Sheng, Y. W., Yao, T. D., Fan, C. J., Li, J. L., Zhao, H., and Lei, Y. B., 2011: Evaporative enrichment of oxygen-18 and deuterium in lake waters on the Tibetan Plateau. *Journal of Paleolimnology*, 46(2): 291–307.

Zhang, G. Q., Yao, T. D., Xie, H. J., Kang, S. C., and Lei, Y. B., 2013: Increased mass over the Tibetan Plateau: From lakes or glaciers? *Geophysical Research Letters*, 40(10): 2125–2130.

Zhang, G. Q., Xie, H. J., Yao, T. D., Li, H. Y., and Duan, S. Q., 2014: Quantitative water resources assessment of Qinghai Lake basin using snowmelt runoff model (SRM). *Journal of Hydrology*, 519: 976–987.

Zhou, S. Q., Kang, S. C., Chen, F., and Joswiak, D. R., 2013: Water balance observations reveal significant subsurface water seepage from Lake Nam Co, south-central Tibetan Plateau. *Journal of Hydrology*, 491: 89–99.

Zhu, L. P., Wu, Y. H., Wang, J. B., Lin, X., Ju, J. T., Xie, M. P., Li, M. H., Mausbache, R., Schwalb, A., and Daut, G., 2008: Environmental changes reflected from the core sediments since 8.4 ka in Nam Co, central Tibet of China. *Holocene*, 18(5): 831–839.

Zhu, L. P., Zhen, X. L., Wang, J. B., Lu, H. Y., Xie, M. P., Kitagawa, H., and Possnert, G., 2009: A ~30,000-year record of environmental changes inferred from Lake Chen Co, southern Tibet. *Journal of Paleolimnology*, 42(3): 343–358.

MS submitted 9 April 2015
MS accepted 25 April 2016

Appendix

TABLE A1

Observed spatial $\delta^{18}O$, δD, and *d*–excess for the long alpine lake Bangong (LBG).

Sampling date (dd/mm/yyyy)	Longitude (°E)	Latitude (°N)	$\delta^{18}O$ (‰)	δD (‰)	*d*–excess (‰)
6/28/2010	79.74	33.48	–4.77	–58	–19.82
6/28/2010	79.72	33.63	–4.63	–50.43	–13.4
6/28/2010	79.72	33.47	–4.54	–56.6	–20.28
6/28/2010	79.93	33.55	–4.38	–50.29	–15.27
6/28/2010	79.76	33.48	–4.02	–48.44	–16.27
6/28/2010	79.89	33.57	–3.5	–45.55	–17.54
6/28/2010	79.82	33.45	–3.5	–44.66	–16.69
6/28/2010	79.85	33.47	–3.45	–44.22	–16.62
6/28/2010	79.75	33.49	–3.41	–43.64	–16.35
6/28/2010	79.76	33.49	–3.39	–43.92	–16.77
6/28/2010	79.89	33.49	–3.09	–42.81	–18.08
6/28/2010	79.66	33.65	–2.53	–40.79	–20.52
6/28/2010	79.9	33.53	–2.51	–42.14	–22.08
6/28/2010	79.62	33.68	–1.29	–34.33	–24.01
6/28/2010	79.47	33.74	–1.07	–33.95	–25.38
6/28/2010	79.56	33.73	–0.38	–30.02	–27.02
6/28/2010	79.37	33.73	0.04	–29.17	–29.51
12/24/2011	79.76	33.49	–4.9	–52.43	–13.22
12/24/2011	79.64	33.66	–4.56	–50.84	–14.37

TABLE A1

Continued

Sampling date (dd/mm/yyyy)	Longitude (°E)	Latitude (°N)	$\delta^{18}O$ (‰)	δD (‰)	*d*–excess (‰)
12/24/2011	79.63	33.67	–4.18	–49.06	–15.58
12/24/2011	79.92	33.57	–4	–47.65	–15.68
12/24/2011	79.83	33.47	–3.92	–47.07	–15.69
12/24/2011	79.8	33.45	–3.87	–46.97	–15.98
12/24/2011	79.84	33.47	–3.87	–46.86	–15.91
12/24/2011	79.89	33.48	–3.84	–46.7	–15.94
12/24/2011	79.92	33.55	–3.83	–46.72	–16.06
12/24/2011	79.81	33.45	–3.81	–46.64	–16.18
12/24/2011	79.87	33.47	–3.79	–46.65	–16.33
12/24/2011	79.57	33.71	–3.24	–44.69	–18.79
12/24/2011	79.18	33.75	–2.05	–39.35	–22.96
12/24/2011	79.31	33.73	–1.41	–35.31	–24
12/24/2011	79.47	33.74	–0.72	–31.62	–25.83
12/24/2011	79.37	33.72	–0.57	–30.9	–26.32
12/24/2011	78.94	33.73	–0.23	–29.37	–27.52
12/24/2011	78.88	33.74	0.57	–24.61	–29.18
12/24/2011	78.91	33.73	0.68	–24.05	–29.5
8/24/2012	79.69	33.63	–3.93	–47.74	–16.28
8/24/2012	79.92	33.57	–3.9	–47.42	–16.2
8/24/2012	79.79	33.44	–3.79	–47.97	–17.61
8/24/2012	79.82	33.45	–3.6	–46.33	–17.52
8/24/2012	79.81	33.45	–3.58	–45.9	–17.24
8/24/2012	79.85	33.47	–3.58	–46.1	–17.45
8/24/2012	79.88	33.57	–3.57	–46.49	–17.93
8/24/2012	79.89	33.49	–3.55	–48.03	–19.62
8/24/2012	79.84	33.47	–3.5	–45.73	–17.71
8/24/2012	79.83	33.47	–3.49	–46.45	–18.54
8/24/2012	79.63	33.66	–3.26	–44.85	–18.8
8/24/2012	79.67	33.6	–2.74	–42.83	–20.44
8/24/2012	79.67	33.64	–2.58	–41.05	–20.4
8/24/2012	79.65	33.64	–2.53	–40.79	–20.56
8/24/2012	79.63	33.67	–2.31	–39.7	–21.23
8/24/2012	79.64	33.67	–2.28	–40.09	–21.88
8/24/2012	79.62	33.67	–2	–38.67	–22.67
8/24/2012	79.63	33.66	–1.98	–39.99	–24.14
8/24/2012	79.6	33.71	–1.54	–36.39	–24.04
8/24/2012	79.59	33.69	–1.43	–35.43	–24.01
8/24/2012	79.1	33.76	–1.25	–35.45	–25.49
8/24/2012	79.58	33.7	–1.06	–34.94	–26.45
8/24/2012	79.55	33.75	–1.04	–38.2	–29.87
8/24/2012	79.09	33.76	–0.87	–33.44	–26.48
8/24/2012	79.18	33.75	–0.82	–32.98	–26.38
8/24/2012	79.12	33.74	–0.71	–31.18	–25.52

TABLE A1

Continued

Sampling date (dd/mm/yyyy)	Longitude (°E)	Latitude (°N)	$\delta^{18}O$ (‰)	δD (‰)	*d*–excess (‰)
8/24/2012	79.47	33.74	–0.6	–32.62	–27.86
8/24/2012	79.32	33.73	–0.44	–30.65	–27.1
8/24/2012	79.43	33.74	–0.43	–30.9	–27.46
8/24/2012	79.25	33.76	–0.39	–31.15	–28.04
8/24/2012	79.31	33.73	–0.37	–30.63	–27.65
8/24/2012	79.37	33.72	–0.35	–30.48	–27.64
8/24/2012	78.95	33.74	–0.3	–30.12	–27.7
8/24/2012	79.41	33.74	–0.26	–30.23	–28.17
8/24/2012	78.96	33.75	–0.07	–28.88	–28.35
8/24/2012	78.94	33.73	0.2	–27.07	–28.65
8/24/2012	78.88	33.74	0.42	–26.11	–29.43
8/24/2012	78.89	33.74	0.67	–24.39	–29.72
8/24/2012	78.93	33.73	0.75	–24.1	–30.09
8/24/2012	78.91	33.73	0.95	–23.28	–30.85